Supplementary Information for

cis-1 Isomers of tethered bismethano [70]fullerene as electron acceptors in organic photovoltaics

Tomokazu Umeyama,[a,*] Shogo Takahara,[a] Sho Shibata,[a] Kensho Igarashi,[a]

Tomohiro Higashino,[a] Kenji Mishima,[b] Koichi Yamashita,[b] and Hiroshi Imahori[a,c,*]

[a]Department of Molecular Engineering, Graduate School of Engineering, Kyoto University, Nishikyo-ku, Kyoto 615-8510, Japan

[b]Department of Chemical System Engineering School of Engineering, The University of Tokyo 7-3-1, Hongo, Bunkyo-ku, Tokyo 113–8656, Japan

[c]Institute for Integrated Cell-Material Sciences (WPI-iCeMS), Kyoto University, Sakyo-ku, Kyoto 606-8501, Japan

e-mail: umeyama@scl.kyoto-u.ac.jp, imahori@scl.kyoto-u.ac.jp

Fax: +81-75-383-2571; Tel: +81-75-383-2568, +81-75-383-2566

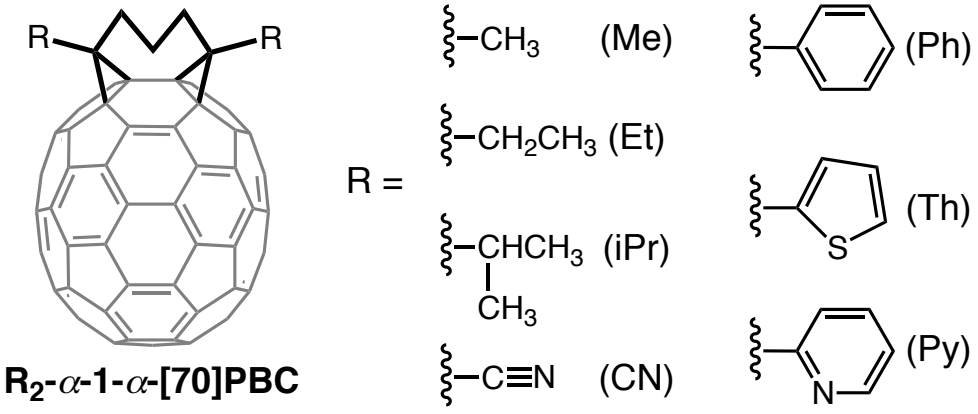

Fig. S1 Structures of R_2-α-1-α-[70]PBC (R = Me, Et, iPr, CN, Ph, Th, Py).

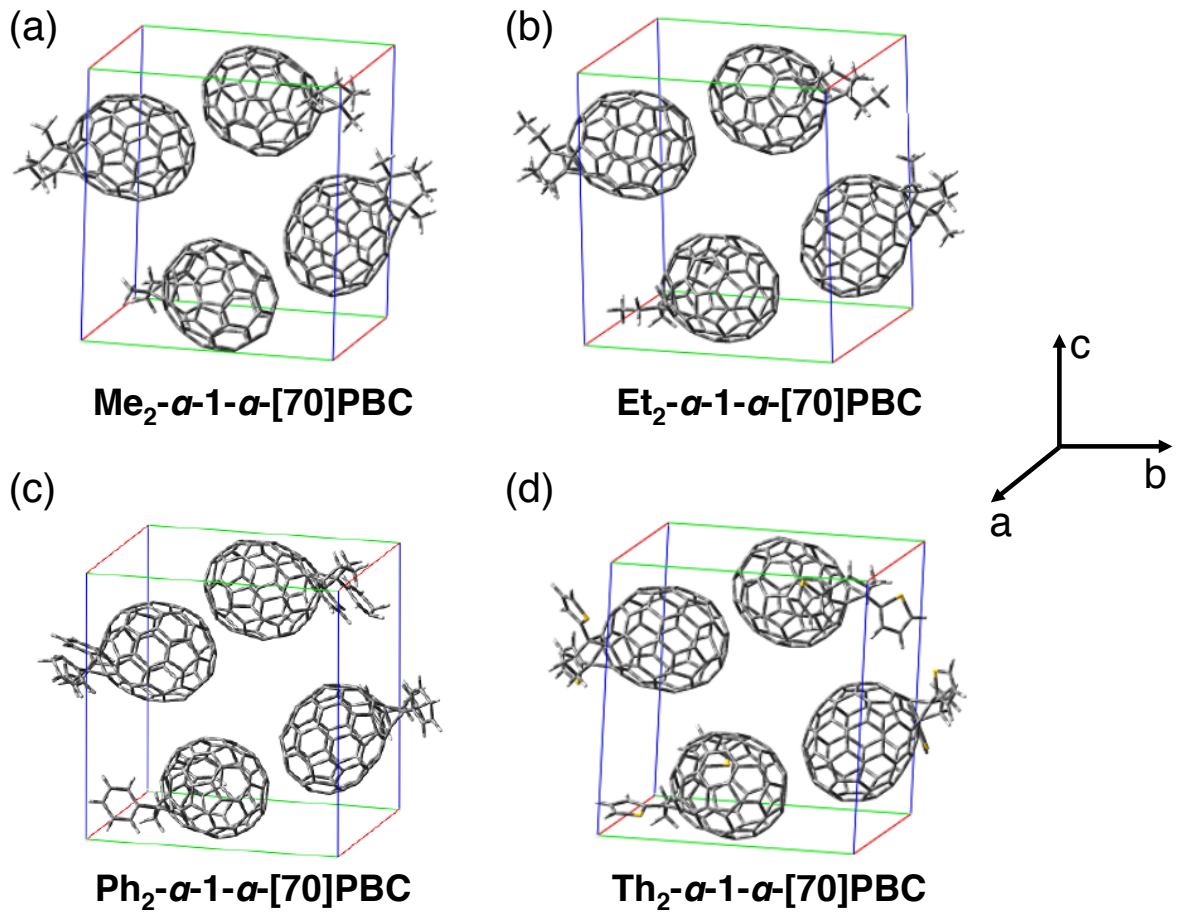

Fig. S2 Representative examples for the structures of R_2-α-1-α-[70]PBC solid systems optimized under periodic boundary conditions at PM6-D3 based on MOPAC. (a) Me_2-α-1-α-[70]PBC, (b) Et_2-α-1-α-[70]PBC, (c) Ph_2-α-1-α-[70]PBC, and (d) Th_2-α-1-α-[70]PBC.

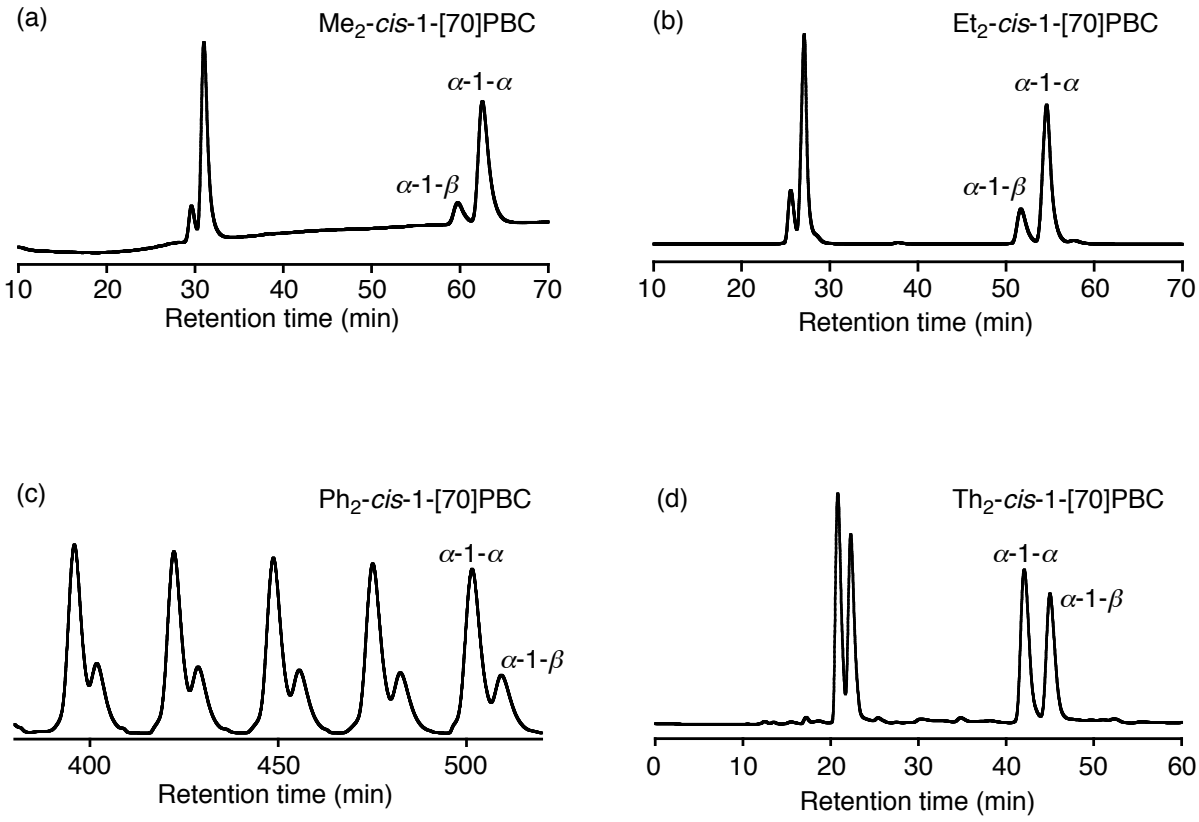

Fig. S3 HPLC profiles with Buckyprep column of (a) Me_2-*cis*-1-[70]PBC, (b) Et_2-*cis*-1-[70]PBC, (c) Ph_2-*cis*-1-[70]PBC, and (d) Th_2-*cis*-1-[70]PBC.

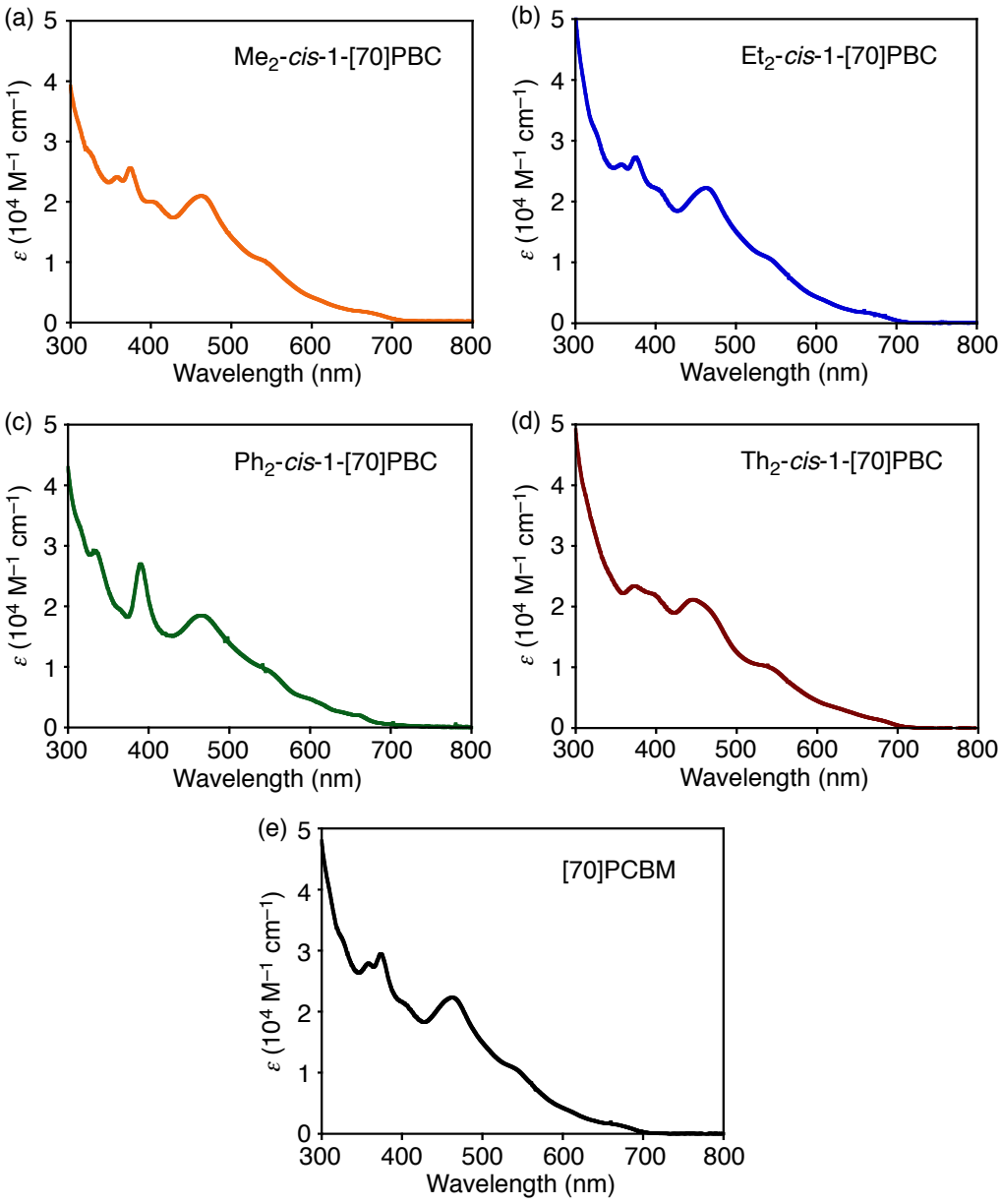

Fig. S4 UV-vis absorption spectra of (a) Me_2-*cis*-1-[70]PBC, (b) Et_2-*cis*-1-[70]PBC, (c) Ph_2-*cis*-1-[70]PBC, (d) Th_2-*cis*-1-[70]PBC, and (e) [70]PCBM in ODCB.

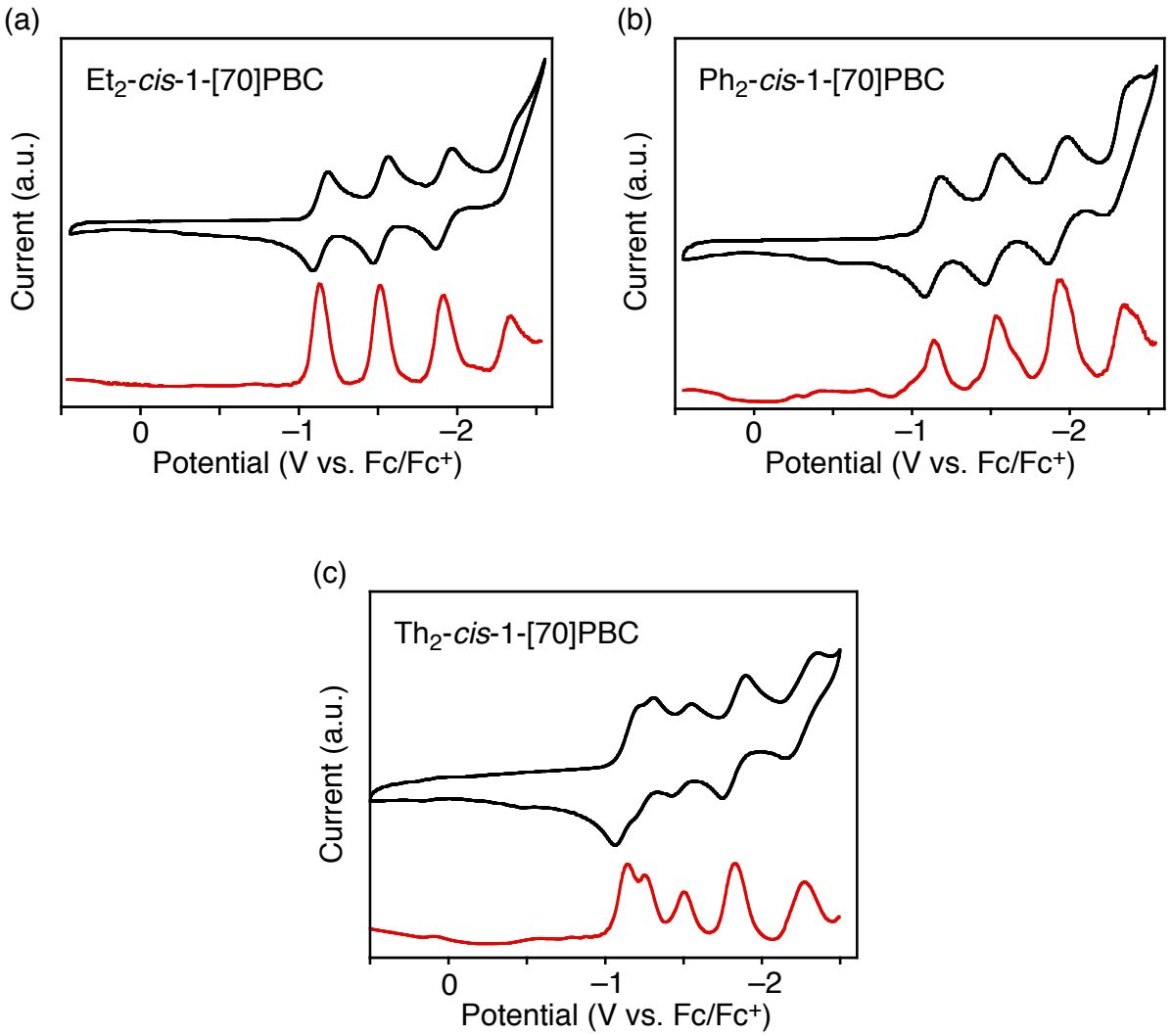

Fig. S5 Cyclic voltammograms (upper) and differential pulse voltammograms (lower) of (a) Et_2-*cis*-1-[70]PBC, (b) Ph_2-*cis*-1-[70]PBC, and (c) Th_2-*cis*-1-[70]PBC versus a reference electrode of Fc/Fc^+ measured in ODCB/acetonitrile mixture (v/v = 5:1) containing 0.1 M tetrabutylammonium hexafluorophosphate (Bu_4NPF_6). Sweep rate: 0.1 V s^{-1}; reference electrode, Ag/Ag^+ (0.01 M $AgNO_3$, 0.09 M Bu_4NPF_6 in acetonitrile).

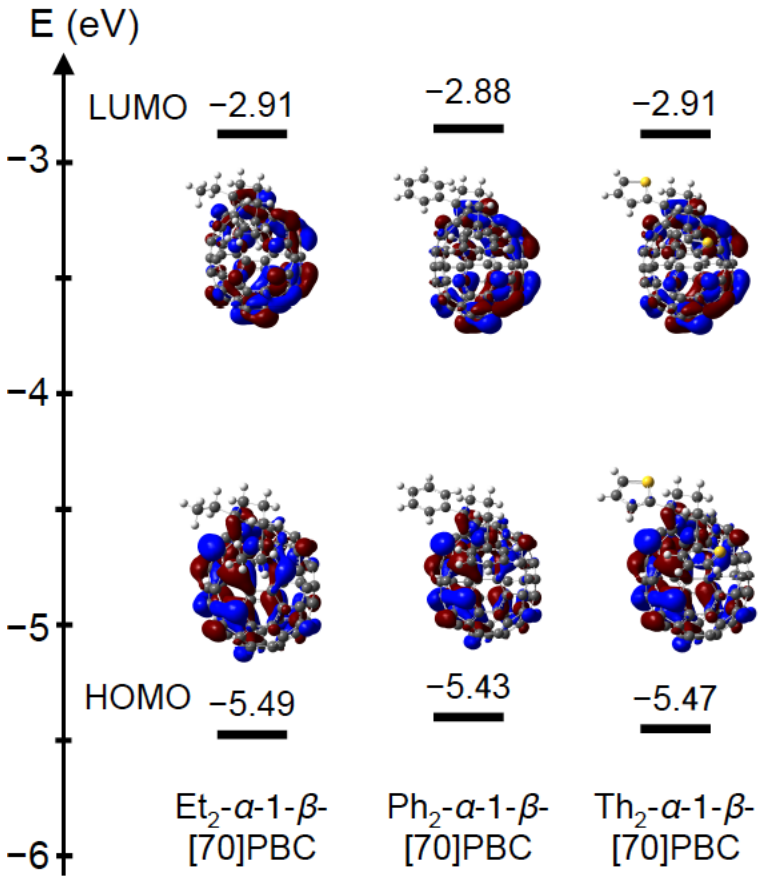

Fig. S6 Optimized geometries, HOMO/LUMO electron density distributions, and energy levels of Et_2-*α*-1-*β*-[70]PBC, Ph_2-*α*-1-*β*-[70]PBC, and Th_2-*α*-1-*β*-[70]PBC by DFT calculations using RB3LYP/6-31G(d) model.

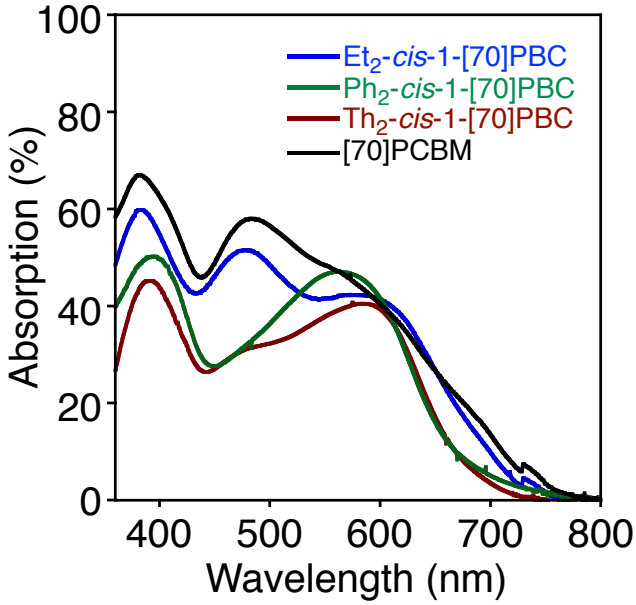

Fig. S7 UV-visible absorption spectra of blend films of PCDTBT:Et_2-*cis*-1-[70]PBC (blue), PCDTBT:Ph_2-*cis*-1-[70]PBC (green), PCDTBT:Th_2-*cis*-1-[70]PBC (brown), and PCDTBT:[70]PCBM (black) on ITO/PEDOT:PSS substrates. Note here that the total absorptions of the ITO/PEDOT:PSS/PCDTBT:fullerene/TiO_x/Al devices are higher than the values in this figure due to the reflection from the Al electrode through the optical spacer, TiO_x.

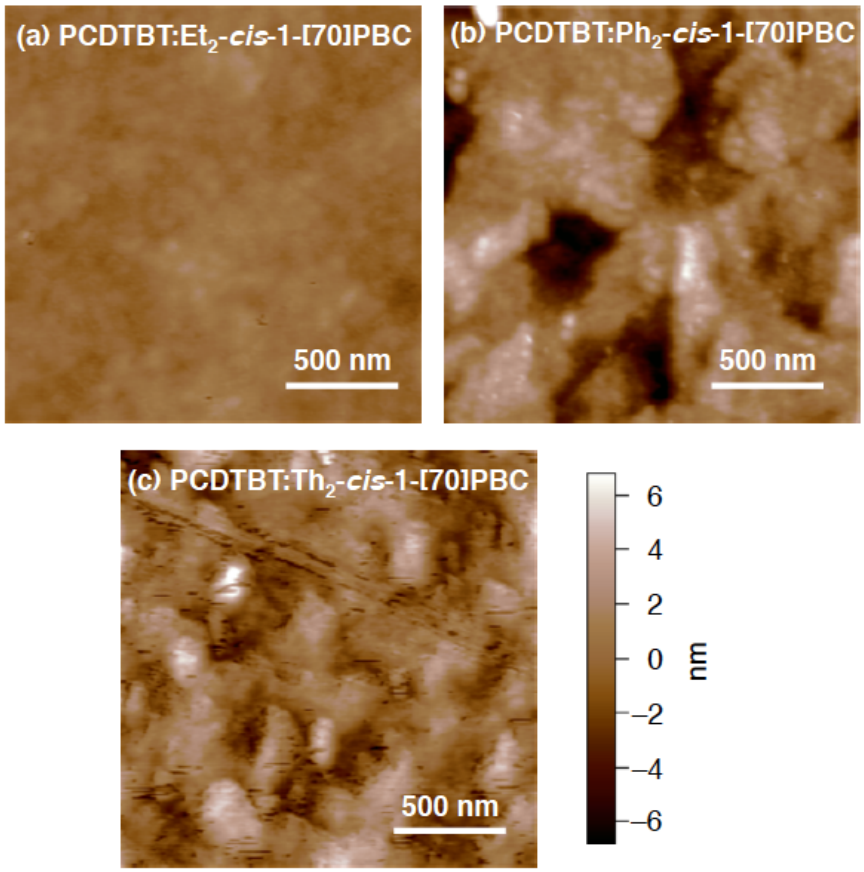

Fig. S8 Tapping-mode atomic force micrographs of ((a) PCDTBT:Et_2-*cis*-1-[70]PBC, (b) PCDTBT:Ph_2-*cis*-1-[70]PBC, and (c) PCDTBT:Th_2-*cis*-1-[70]PBC on ITO/PEDOT:PSS substrates. The color scale represents the height topography, with bright and dark representing the highest and lowest features, respectively. The rms surface roughnesses are (a) 0.59, (b) 2.3, and (c) 1.9 nm, respectively.

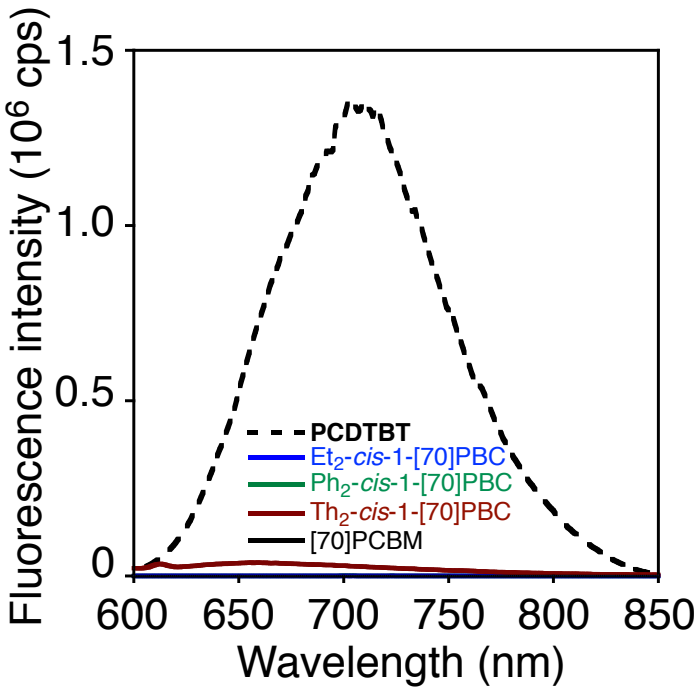

Fig. S9 Photoluminescence spectra of PCDTBT single component film (black dotted line) and blend films of PCDTBT with Et_2-*cis*-1-[70]PBC (blue solid line), Ph_2-*cis*-1-[70]PBC (green solid line), Th_2-*cis*-1-[70]PBC (brown solid line), and [70]PCBM (black solid line). The excitation wavelengths are 540 nm. The emission intensities were normalized by that of the PCDTBT film considering the difference in the absorbances of the PCDTBT:fullerene films at the excitation wavelength.

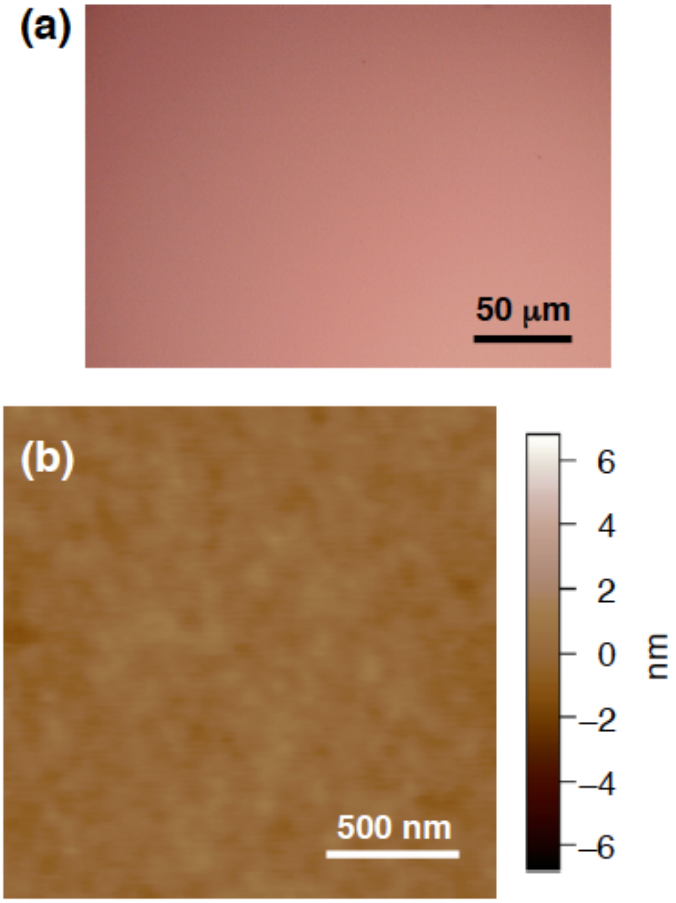

Fig. S10 (a) Optical microscopy image and (b) tapping-mode atomic force micrograph of PCDTBT:[70]PCBM on ITO/PEDOT:PSS substrates. In (b), the color scale represents the height topography, with bright and dark representing the highest and lowest features, respectively. The rms surface roughness is 0.35 nm.

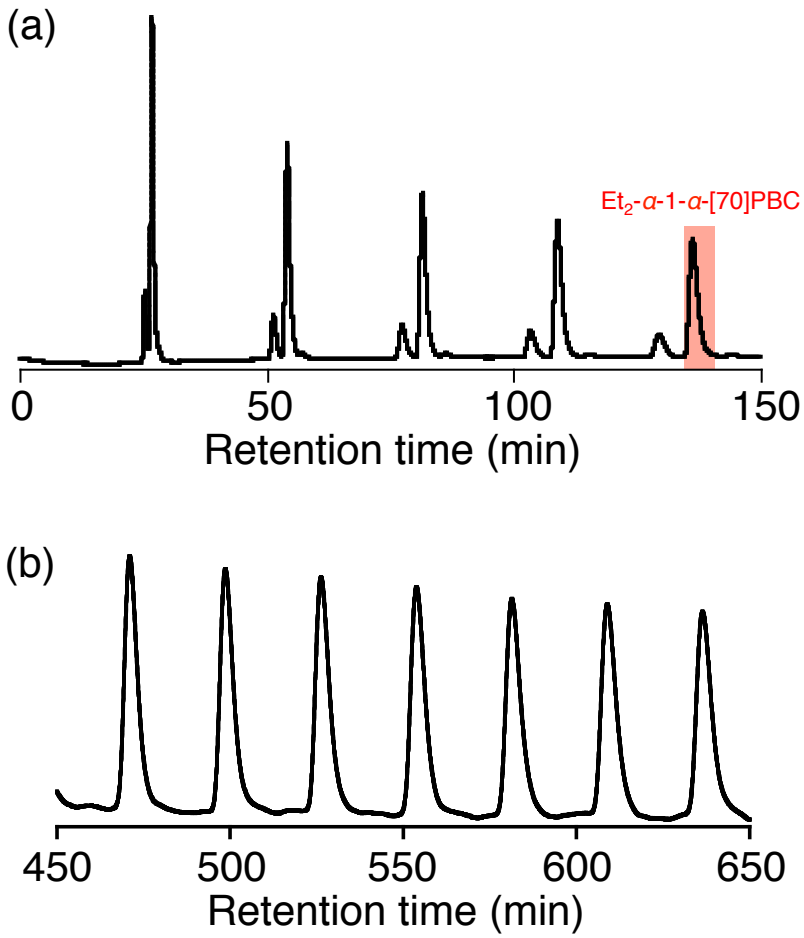

Fig. S11 (a) HPLC profile with 5PBB column of Et_2-*cis*-1-[70]PBC. The fraction marked with red color was collected and assigned to Et_2-*α*-1-*α*-[70]PBC. (b) HPLC profile with 5PBB column of Et_2-*α*-1-*α*-[70]PBC.

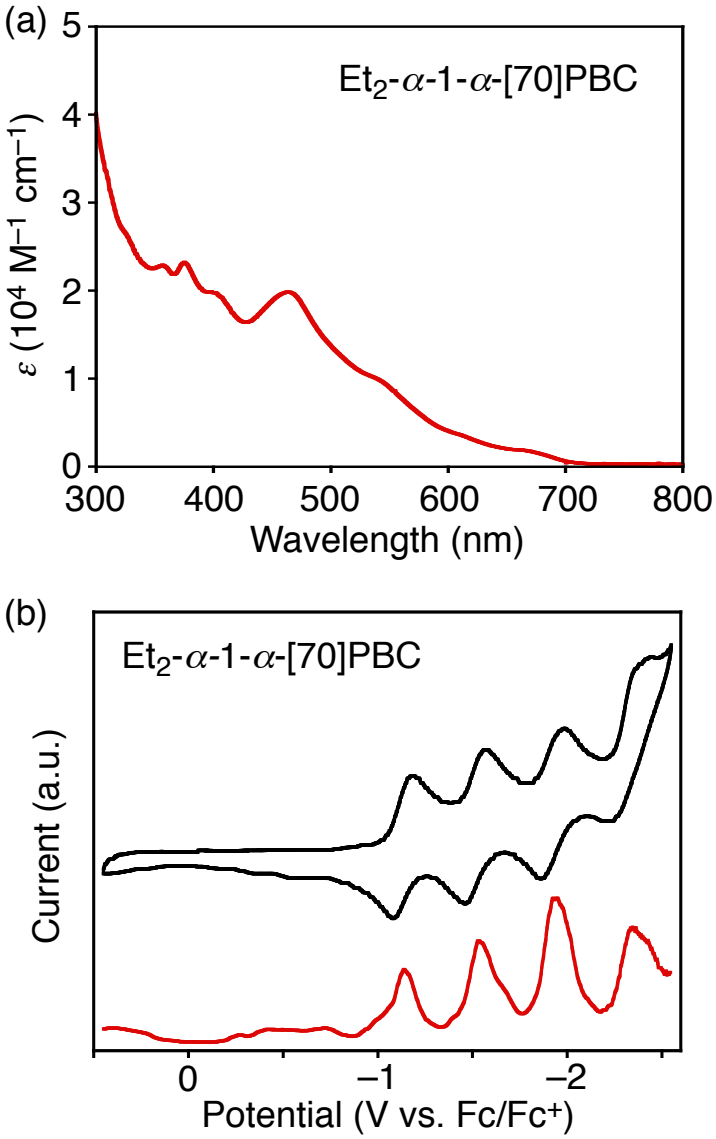

Fig. S12 (a) UV-vis absorption spectrum of Et_2-α-1-α-[70]PBC in ODCB. (b) Cyclic voltammogram (upper) and differential pulse voltammogram (lower) of Et_2-α-1-α-[70]PBC versus a reference electrode of Fc/Fc^+ measured in ODCB/acetonitrile mixture (v/v = 5:1) containing 0.1 M tetrabutylammonium hexafluorophosphate (Bu_4NPF_6). Sweep rate: 0.1 V s^{-1}; reference electrode, Ag/Ag^+ (0.01 M $AgNO_3$, 0.09 M Bu_4NPF_6 in acetonitrile).

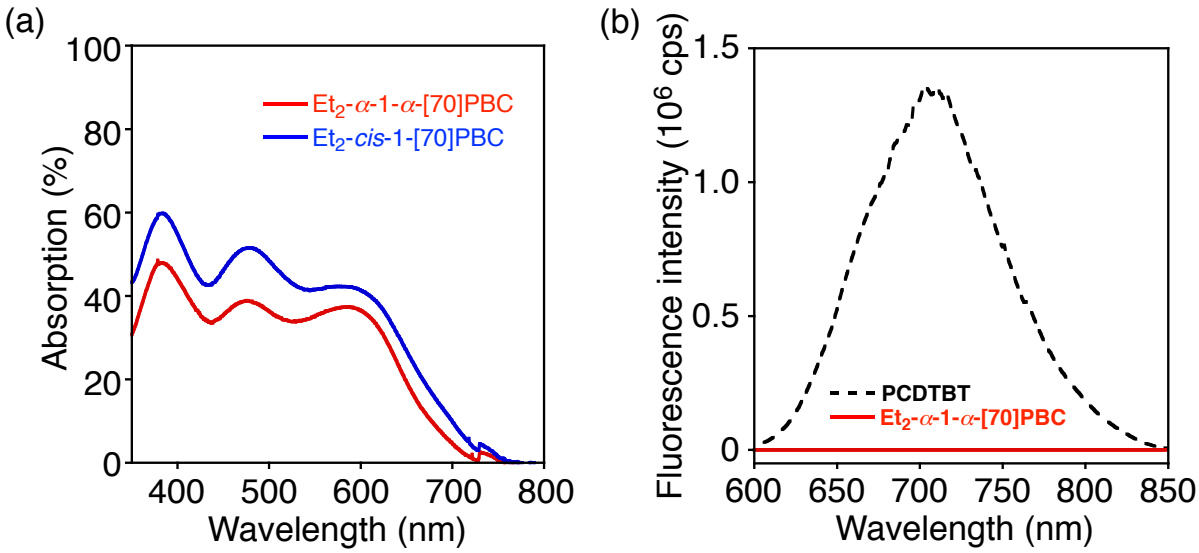

Fig. S13 (a) UV-visible absorption spectra of blend films of PCDTBT:Et_2-α-1-α-[70]PBC (red) and PCDTBT:Et_2-*cis*-1-[70]PBC (blue). (b) Photoluminescence spectra of PCDTBT single component film (black dotted) and PCDTBT:Et_2-α-1-α-[70]PBC (red). The excitation wavelengths are 540 nm. The emission intensities were normalized by that of the PCDTBT film considering the difference in the absorbances of the PCDTBT:Et_2-α-1-α-[70]PBC film at the excitation wavelength.

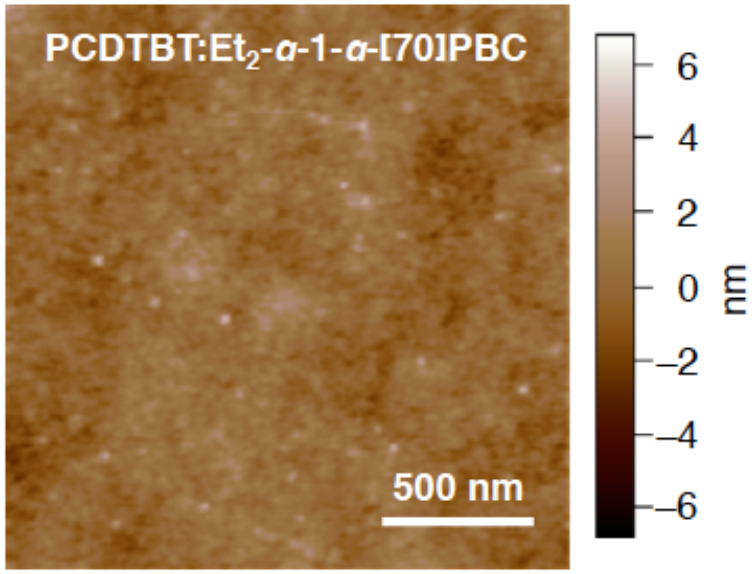

Fig. S14 Tapping-mode atomic force micrographs of PCDTBT:Et_2-α-1-α-[70]PBC on ITO/PEDOT:PSS substrates. The color scale represents the height topography, with bright and dark representing the highest and lowest features, respectively. The rms surface roughness is 0.78 nm.